violet region, some insight can be gained concerning the cis–trans isomerism in complexes of this type.

Registry No. Ni(D-Ala)$_2$·2H$_2$O, 39732-80-4; Ni(L-Val)$_2$·2H$_2$O, 39732-81-5; Ni(L-Ile)$_2$·2H$_2$O, 39732-82-6; Ni(L-Pro)$_2$·2H$_2$O, 39732-83-7; Na$_2$[Ni(D-Asp)$_2$]·5H$_2$O, 39708-44-6; Ni(D-Aspar)$_2$·1.5H$_2$O, 37343-98-9; Ni(L-His)$_2$·H$_2$O, 32424-04-7; Ni(L-Ser)$_2$·3.5H$_2$O, 39732-85-9; Ni(L-Ala)$_2$·2H$_2$O, 22585-12-2; [Ni(D-Aspar)$_2$]·2H$_2$O, 37343-99-0; [Ni(L-ornithine)$_2$]·2HCl, 39732-87-1.

Acknowledgment. The authors are grateful to the National Research Council of Canada for financial support of this work.

Contribution from the Department of Chemistry, Brandeis
University, Waltham, Massachusetts 02154

Anomalous Complexation Kinetics of Transition Metal Ions with L-Dopa (3,4-Dihydroxyphenylalanine). Kinetics and Complex Formation with Nickel(II) and Cobalt(II)[1]

MORTON L. BARR, KENNETH KUSTIN,* and SUNG-TSUEN LIU

Received January 22, 1973

The temperature-jump relaxation method has been used to determine the complexation rate constants for the reactions of L-dopa (amino acid end) with nickel(II) and cobalt(II) at 25° and 0.1 *M* ionic strength. The complexation reactions observed are of the type $M^{2+} + H_2L^- \rightleftarrows MH_2L^+$, where H_2L^- is the anionic form of the ligand, in which both hydroxyl groups are protonated. The rate constants for this reaction are $k_1 = 2.2\ (\pm 0.3) \times 10^3\ M^{-1}\ \mathrm{sec}^{-1}$ and $k_{-1} = 3.1\ (\pm 0.8) \times 10^{-2}\ \mathrm{sec}^{-1}$ for $M^{2+} = Ni^{2+}$; $k_1 = 4.3\ (\pm 0.3) \times 10^5\ M^{-1}\ \mathrm{sec}^{-1}$ and $k_{-1} = 72\ (\pm 7)\ \mathrm{sec}^{-1}$ for $M^{2+} = Co^{2+}$. The association rate constants are low compared with normal substitution values. This effect is attributed to misorientation of the ligand in the ion-pair complex by hydrogen bonding. The complex NiH_2L^+ can also undergo reaction according to $NiH_2L^+ \rightleftarrows NiHL + H^+$, for which $k_D = 1\ (\pm 1)\ \mathrm{sec}^{-1}$ and $k_H = 6.9\ (\pm 0.4) \times 10^7\ M^{-1}\ \mathrm{sec}^{-1}$. The bimolecular protolytic reaction is several orders of magnitude slower than the diffusion-controlled limit. The necessary equilibrium constants were determined by potentiometric pH titration. The measured acid dissociation constants of L-dopa are $pK_{a2}(\text{-}NH_3^+) = 8.76 \pm 0.03$, $pK_{a3}(\text{-}OH) = 9.89 \pm 0.02$; and the stability constants are as follows: Ni^{2+}, $\log K_1 = 4.85 \pm 0.04$, $\log K_2 = 4.28 \pm 0.04$; Co^{2+}, $\log K_1 = 3.75 \pm 0.03$, $\log K_2 = 3.50 \pm 0.04$.

Transition metal ion–α-amino acid complexes are generally formed *via* a mechanism in which the rate-determining step is the loss of a water molecule from the metal ion's inner coordination sphere.[2,3] For normal substitution, ligand penetration into the inner coordination sphere of the metal ion is essentially independent of ligand characteristics.[2]

Recent kinetic investigations into the reactions of Cu^{2+}, Co^{2+}, and Ni^{2+} with hydroxyproline[4] and of Cu^{2+} with L-dopa (3,4-dihydroxyphenylalanine)[5] indicate that the addition of a single hydroxyl group suitably oriented on the parent amino acid (proline[4] and tyrosine,[6] respectively) has a pronounced effect on the rates of metal substitution reactions. Forward substitution rate constants for these metal–ligand systems are from one-third to one-tenth smaller than rate constants observed for normal systems, as in the cases of proline and tyrosine. The distinguishing feature of these anomalously slow complexation reactions is that the effect is comparable for Cu^{2+}, Co^{2+}, and Ni^{2+}, suggesting that the slower reaction rates are not due to a shift to another rate-determining step, such as closure of the chelate ring.[7-9]

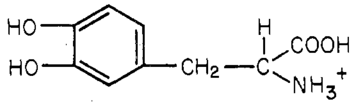

dopa, fully protonated = H_4L^+

The present investigation into L-dopa complexation with Ni^{2+} and Co^{2+} was undertaken in the search of more evidence for interaction between the ligand hydroxyl groups and metal ions.

Experimental Section

Reagent grade $Ni(NO_3)_2 \cdot 6H_2O$ and $Co(NO_3)_2 \cdot 6H_2O$ (Fisher), KNO_3 (Baker), L-dopa (Nutritional Biochemicals Corp.), and Chlorophenol Red and Methyl Red (Eastman) were used without further purification.

Stock solutions of KNO_3, metal nitrates, and indicators were prepared by weight. The metal content of the stock solutions was determined by passing aliquots of the solutions through a cation exchanger (Dowex 50) and titrating the liberated acid with standardized sodium hydroxide solution. Solutions to be studied were prepared by mixing the desired volumes of stock solutions with weighed amounts of solid L-dopa in 100-ml volumetric flasks. (Stock solutions of L-dopa were unstable at neutral pH, turning brown after several hours.) The solutions were degassed and then transferred to a double-walled cell of approximately 200-ml capacity. The cell

---

[1] The authors gratefully acknowledge support from Public Health Service Research Grant GM-08893-11 from the National Institute of General Medical Sciences, Public Health Service.

[2] (a) M. Eigen and R. G. Wilkins, *Advan. Chem. Ser.*, No. 49, 55 (1965); (b) F. Basolo and R. G. Pearson, "Mechanisms of Inorganic Reactions," 2nd ed, Wiley, New York, N. Y., 1967.

[3] K. Kustin and J. Swinehart, *Progr. Inorg. Chem.*, 13, 107 (1970).

[4] K. Kustin and S. T. Liu, *J. Chem. Soc., Dalton Trans.*, 278 (1973).

[5] R. L. Karpel, K. Kustin, A. Kowalak, and R. F. Pasternack, *J. Amer. Chem. Soc.*, 93, 1085 (1971).

[6] M. L. Barr, E. Baumgartner, and K. Kustin, *J. Coord. Chem.*, in press.

[7] W. B. Makinen, A. F. Pearlmutter, and J. E. Stuehr, *J. Amer. Chem. Soc.*, 91, 4083 (1969).

[8] K. Kustin, R. F. Pasternack, and E. M. Weinstock, *J. Amer. Chem. Soc.*, 88, 4610 (1966).

[9] A. Kowalak, K. Kustin, R. F. Pasternack, and S. Petrucci, *J. Amer. Chem. Soc.*, 89, 3126 (1967).

was fitted with inlets for oxygen-free nitrogen gas and electrodes. In kinetic studies, the pH was adjusted by dropwise addition of dilute NaOH and/or HNO_3. The final pH value was measured to ±0.02 pH unit on a Radiometer TTT1c titrator assembly (Copenhagen) used as a pH meter. To prevent inclusion of atmospheric oxygen, the solutions were transferred carefully to the temperature-jump cell, which was then flushed with nitrogen gas and sealed. (Air oxidation of L-dopa solutions is a consistent problem above pH 6 and appears to be catalyzed by excess metal ion.) Hydrogen ion concentrations were obtained by dividing the measured hydrogen ion activity by $\gamma_\pm = 0.739$ from the Davies equation.[10] The temperature in all kinetic experiments was 25 ± 1°.

The temperature-jump apparatus described in a previous paper was modified,[11] permitting easier and more accurate measurement of relaxation times. The output from the photomultiplier–impedance transformer circuit is captured by a Biomation 610B transient recorder. Voltage *vs.* time data are obtained from the 610B on paper tape with a 33ASR Teletype equipped with a Pivan Dijitscan B103 interface. Output to an oscilloscope with this arrangement is also possible; samples are shown in Figure 1. Relaxation times are calculated by least-squares analysis of the voltage–time data on a DEC PDP-10 computer.

Blank experiments with Co^{2+} and indicator and with L-dopa and indicator gave no discernible relaxation effects. Solutions of nickel and indicator, however, showed relatively small effects in the pH and time ranges studied and are attributed to complexation with the indicator. This interference was circumvented by making certain the blank effect was negligible compared with the desired effect (typical relaxation times for the blank effects are longer than 100 msec).

In determining the stability constants of the complexes and the acid dissociation constants for L-dopa, the double-walled cell previously mentioned was used. An additional inlet was used for a 2-ml capacity Gilmont microburet. The temperature of the solutions was kept at 25 ± 0.1° by circulating water from a thermostated temperature bath through the wall of the cell. The glass electrode was calibrated with standard buffer solutions and checked before and after each titration. The solutions introduced into the cell were in stoichiometric ratios of 6:1, 3:1, and 1:10 ligand to metal.

Results and Discussion

Relaxation Spectra. The experimental conditions were chosen so that only the mono-L-dopa complexes of the metal ions would be present. The relaxation times, τ, were calculated from standard expressions,[12] using stoichiometric equilibrium constants (Table I) and concentrations (Table II). The experimental relaxation times listed in Table II were obtained by averaging at least four experimental values of τ as described in the Experimental Section. The deviations were usually less than ±10% in these averaged relaxation times. The exponentiality of the effects was confirmed by semilogarithmic plots of voltage *vs.* time.

Nickel. Under the experimental conditions of this study—acid pH, appreciable free nickelous ion—the complete reaction scheme is

$$Ni^{2+} + H_2L^- \underset{k_{-1}}{\overset{k_1}{\rightleftharpoons}} NiH_2L^+ \underset{k_H}{\overset{k_D}{\rightleftharpoons}} NiHL + H^+ \qquad (1)$$

Other protonated forms of L-dopa exist in these solutions; but, as is the case with other amino acids,[3] only anionic forms of the ligand attack the metal ion. On the other hand, in this pH range, L-dopa forms only amino acid type complexes.[13] Reaction scheme 1 is characterized by two relaxation processes, separable in time by two to three orders of magnitude (Figure 1). The faster effect, the relaxation time of which decreases with increasing hydrogen ion concentration, has been assigned to the reaction $NiH_2L^+ \rightleftharpoons NiHL + H^+$. In the limiting case of widely separable relaxation times, the relaxation expression for this process is

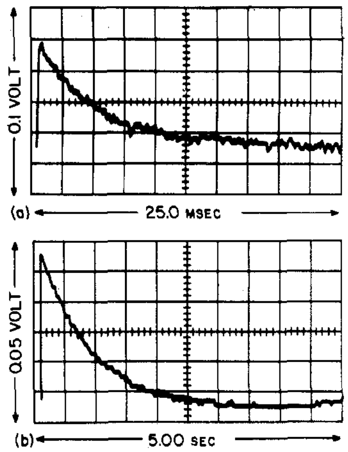

Figure 1. Relaxation spectra for nickel(II)–L-dopa solutions. The oscillographs were obtained from the output of a Biomation 610B transient recorder as displayed on a Tektronix 549 storage oscilloscope. The total elapsed time shown on the abscissa represents real time and not the sweep time of the oscilloscope, which is the same in both (a) and (b). (a) $[Ni^{2+}]_0 = 1.00 \times 10^{-2}$ *M*, $[\text{L-dopa}]_0 = 1.00 \times 10^{-3}$ *M*, pH 5.75, $\tau = 4.3$ msec. (b) Same conditions as (a), $\tau = 8.5 \times 10^{-1}$ sec.

Table I. Equilibrium Data 25° and 0.1 *M* Ionic Strength

Acid Dissociation of L-Dopa

pK_{1a} (-COOH)	pK_{2a} ($-NH_3$)	pK_{3a} (-OH)	pK_{4a} (-OH)	pK_M (-OH)
2.31[a]	8.76 (±0.03)	9.89 (±0.02)	13.4[a]	7.7 (±0.3)

Stability Constants of L-Dopa–Metal Complexes

Metal ion	log K_1	log K_2
Ni(II)	4.85 (±0.04)	4.28 (±0.04)
Co(II)	3.75 (±0.03)	3.50 (±0.04)

Acid Dissociation of Indicators[b]

Indicator	K_{In}, *M*
Chlorophenol Red	1.00×10^{-6}
Methyl Red	1.00×10^{-5}

[a] Reference 13b. [b] I. M. Kolthoff, *J. Phys. Chem.*, 34, 1466 (1930).

$$\frac{1}{\tau_1} = k_D + k_H \left\{ \frac{[NiHL]}{1 + \dfrac{[In] + [H^+] + K_{In}}{[H^+] + K_{In}}} + [H^+] \right\} \qquad (2)$$

Terms in the denominator arising from coupling of H^+ to the free forms of the ligand have been omitted from (2) as they are smaller than the other terms. Values of k_H and k_D can be obtained by plotting eq 2, as shown in Figure 2.

However, in order to calculate the concentration of NiHL, especially, it is necessary to know the value of the acid dissociation constant, K_M, for $NiH_2L^+ \rightleftharpoons NiHL + H^+$, which is unknown. Therefore, guess values of K_M were used in calculating the equilibrium concentrations of species present. Values of [NiHL] obtained in this way were used to calculate k_H and k_D. The new value $K_M = k_D/k_H$ was then used in iteration of this procedure until we obtained constancy of experimental *vs.* calculated values of the relaxation times for the best fit. The unknown constants determined by this procedure are $k_H = 6.9\ (\pm 0.4) \times 10^7\ M^{-1}\ \text{sec}^{-1}$, $k_D = 1\ (\pm 1)\ \text{sec}^{-1}$, and $K_M = 2\ (\pm 1) \times 10^{-8}\ M$. The bimolecular rate constant k_H is several orders of magnitude lower than the diffusion-controlled limit.

---

(10) C. W. Davies, *J. Chem. Soc.*, 2093 (1938).

(11) P. Hurwitz and K. Kustin, *Inorg. Chem.*, 3, 823 (1964).

(12) (a) G. G. Hammes and J. I. Steinfeld, *J. Amer. Chem. Soc.*, 84, 4639 (1962); (b) I. Amdur and G. G. Hammes, "Chemical Kinetics," McGraw-Hill, New York, N. Y., 1966, pp 141-142.

(13) (a) J. E. Gorton and R. F. Jameson, *J. Chem. Soc., Dalton Trans.*, 3, 310 (1972); (b) J. E. Gorton and R. F. Jameson, *J. Chem. Soc. A*, 2615 (1968).

Table II. Relaxation Spectra of L-Dopa–Metal Complexes[a,b]

$10^3 \times [Ni(II)]_0$,[c] M	10^3[L-dopa], M	pH	Exptl τ_1, msec	Exptl τ_2, sec	Calcd τ_1, msec	Calcd τ_2, sec
1.00	0.51	5.75	4.9	1.5	5.0	1.4
1.00	0.20	5.74	6.8		5.4	
1.00	1.00	5.75	4.3	0.85	4.3	0.83
2.00	1.01	5.75	3.3	0.59	3.7	0.59
1.00	1.00	5.97	4.9	0.62	4.3	0.68
2.00	1.02	5.95	3.8	0.60	3.5	0.55
1.00	0.55	5.97	5.3	0.86	5.7	0.89
1.00	1.02	5.54	3.3	0.89	3.3	
2.00	1.04	5.54	3.0	0.81	3.1	0.84
1.01	0.54	5.53	2.8	1.2	3.4	
1.01	1.02	5.29	2.0		2.0	
1.00	1.05	5.14	1.5		1.4	

$10^3[Co(II)]_0$,[d] M	10^4[L-dopa]$_0$, M	pH	Exptl τ_1, msec	Calcd τ_1, msec
4.05	1.20	5.92	9.0	8.6
8.09	1.20	5.98	6.0	5.8
2.02	1.20	5.89	9.9	10.8
6.07	2.45	5.57	8.7	8.3
1.01	1.23	5.61	14.7	13.1
3.27	5.52	5.84	4.9	5.3
6.37	5.59	5.84	3.3	3.3
2.54	22.5	5.38	6.7	7.0
5.27	6.74	5.83	3.5	3.5

[a] The subscript 0 refers to total stoichiometric concentration. [b] Temperature 25°; ionic strength 0.1 M (KNO_3). [c] Monitored with Methyl Red, 1.6×10^{-5} M. [d] Monitored with Chlorophenol Red, 1.4×10^{-5} M.

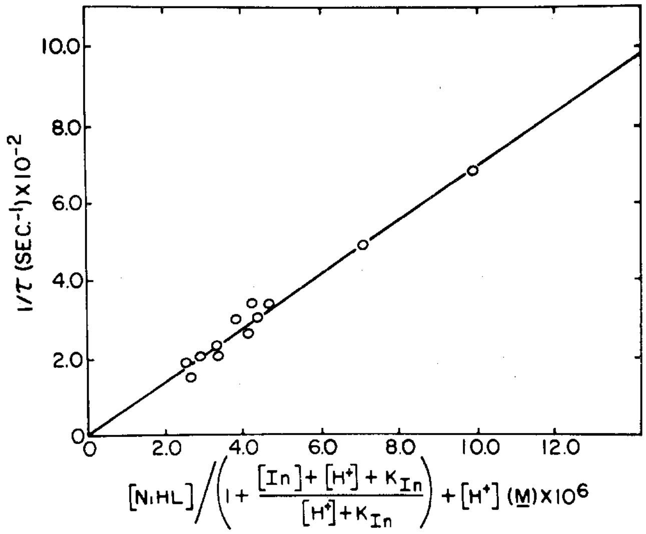

Figure 2. Plot of $1/\tau_1$ *vs.*

$$[NiHL]/\left(1 + \frac{[In] + [H^+] + K_{In}}{[H^+] + K_{In}}\right) + [H^+]$$

The straight line was obtained by least-squares analysis of the data, calculated from the concentrations and relaxation times given in Table II.

The slower relaxation time increases with increasing hydrogen ion concentration; it has been assigned to $Ni^{2+} + H_2L^- \rightleftarrows NiH_2L^+$, for which

$$1/S\tau_2 = k_{-1} + k_1R/S \qquad (3)$$

Unlike the shorter relaxation time, τ_2 is strongly coupled to the indicator and ligand protolytic equilibria,[12a] and to the faster process, as well.[12b] The factors R and S are given in the Appendix. Plotting eq 3 yields $k_1 = 2.2\ (\pm 0.3) \times 10^3\ M^{-1}\ sec^{-1}$. The reverse rate constant, k_{-1}, is unobtainable from Figure 3 and was calculated from the relation $k_{-1} = k_1/K_1$; $k_{-1} = 3.1\ (\pm 0.8) \times 10^{-2}\ sec^{-1}$.

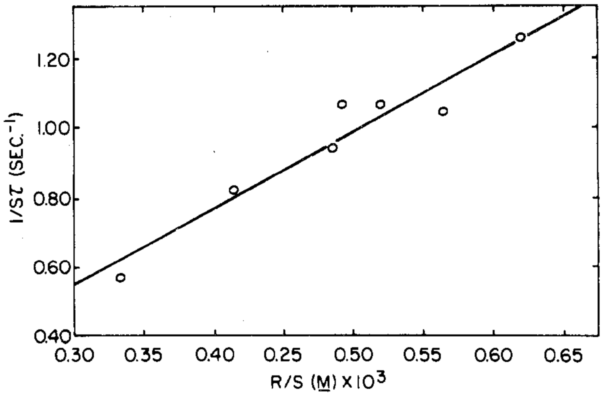

Figure 3. Plot of $1/S\tau_2$ *vs.* R/S. Seven of nine points were used in least-squares analysis of the data, calculated from the concentrations and relaxation times given in Table II.

Cobalt. Only one relaxation time was observed for the Co^{2+}-dopa system. The experimental data can best be described by the reaction scheme

$$Co^{2+} + H_2L^- \underset{k_{-1}}{\overset{k_1}{\rightleftarrows}} CoH_2L^+ \qquad (4)$$

according to

$$1/\tau = k_{-1} + k_1([Co^{2+}]/[1 + \alpha] + [H_2L^-]) \qquad (5)$$

where the α term is also given in the Appendix. From the slope of a plot of eq 5 (Figure 4), $k_1 = 4.3\ (\pm 0.3) \times 10^5\ M^{-1}\ sec^{-1}$ and from the intercept, $k_{-1} = 72\ (\pm 7)\ sec^{-1}$. The ratio of these two quantities, $K_1 = 6.0 \times 10^3\ M^{-1}$, is in good agreement with the value of $5.6 \times 10^3\ M^{-1}$ obtained by potentiometric titration.

Rate constants for L-dopa with divalent nickel, cobalt, and copper are listed in Table III and compared with values for L-tyrosine (p-hydroxyphenylalanine).

Although there is no *a priori* reason to exclude the reaction $M^{2+} + HL^{2-} \rightleftarrows MHL$, the lack, within experimental error, of an observable pH dependence of the type produced by two or more attacking species excludes reaction pathways *via* hydrolytic species such as MOH^+, or other forms of the ligand. In addition, the zwitterions of a large number of amino acids and pyridinecarboxylates have been shown not to be attacking species.[14]

Stability Constants. Values of the stepwise stability constants for cobalt(II)- and nickel(II)-L-dopa complexes and the pertinent acid dissociation constants of L-dopa were determined by potentiometric pH titration. The results are given in Table I. The species in which both hydroxyl groups are deprotonated was not considered, as its pK of approximately 13 leads to a negligibly small concentration.

In the method used for these determinations, values of $\bar{n}$, the average number of ligand molecules bound per metal ion,[15] and $[H_2L^-]$ were obtained for each point along the titration curve. (For pK_a determinations, the average number of protons bound per ligand molecule, $\bar{h}$, and $[H^+]$ were the corresponding variables.) One, two, or three parameters were adjusted in a nonlinear least-squares program (ORGLS),[16] run on a DEC PDP-10 computer, to find the best fit of calculated *vs.* experimental values of $\bar{n}$ or $\bar{h}$.

---

(14) J. C. Cassatt and R. G. Wilkins, *J. Amer. Chem. Soc.*, **90**, 6045 (1968).

(15) F. Rossotti and H. Rossotti, "The Determination of Stability Constants," McGraw-Hill, New York, N. Y., 1961, Chapter 5.

(16) W. R. Busing and H. A. Levy, Report ORNL-TM-271, Oak Ridge National Laboratories Least-Squares Program, Oak Ridge National Laboratory, Oak Ridge, Tenn., 1962.

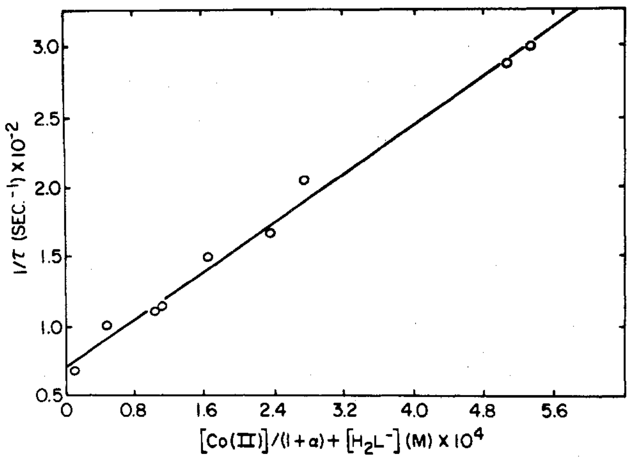

Figure 4. Plot of $1/\tau$ *vs.* $[Co(II)]/(1 + \alpha) + [H_2L^-]$. The straight line was obtained by least-squares analysis of the data, calculated from the concentrations and relaxation times given in Table II.

Table III. Rate Constants of Transition Metal Ions with L-Dopa and L-Tyrosine[a]

Metal ion	k_1, M^{-1} sec^{-1}	k_{-1}, sec^{-1}	k_H, M^{-1} sec^{-1}	k_D, sec^{-1}
		L-Dopa		
Ni(II)	2.2 (±0.3) × 10^3	3.1 (±0.8) × 10^{-2}	6.9 (±0.4) × 10^7	1 (±1)
Co(II)	4.3 (±0.3) × 10^5	72 (±7)		
Cu(II)[b]	1.1 × 10^8	8.3		
		L-Tyrosine		
Ni(II)	1.4 × 10^4	0.10		
Co(II)	1.3 × 10^6	1.1 × 10^2		
Cu(II)	1.1 × 10^9	14		

[a] Reference 6. [b] Reference 5.

Inclusion of the deprotonation equilibrium of NiH_2L^+ invalidates application of the above procedure. This problem arises only with nickel. However, knowledge of the approximate value of K_M from the temperature-jump experiments has enabled us to select those conditions for the stability constant determination, in which interference from NiHL complexes can be minimized. Furthermore, in the nickel determination, a titration with $[Ni^{2+}]_0/[\text{L-dopa}]_0 = 10$ was performed in the pH interval 4.6–6.5 to ensure the most reliable measure of K_1. The validity of this approach was tested nomographically, by plotting $\bar{n}/(1 - \bar{n})$ against $[H_2L^-]$;[15] the plot should be linear, as was the case. The results reported in Table I are in reasonable agreement with those previously determined at the higher ionic strength of 1 M.[13] The maximum relative errors in these constants are ±10%.

In acidic to neutral solutions, L-dopa forms five-membered ring amino acid type complexes with the first-row divalent transition metal ions.[12] For the normal dissociative mechanism of substitution, $k_1 = k_0K_{ip}$, where k_0 is the water-exchange rate constant (sec^{-1}) and K_{ip} is the ion-pair formation constant (M^{-1}). As Table III shows, the L-dopa values are approximately 0.15, 0.33, and 0.10 times smaller than the corresponding tyrosine values for nickel, cobalt, and copper, respectively. The decrease in rate constant for complex formation cannot, therefore, arise from a shift to a new, rate-determining step, as then the factor would decrease monotonically from nickel to copper, being as small as 0.02 for the latter.[3] Normal substitution prevails, and k_1 can be understood in terms of the well-known two-step mechanism denoted above.

In a previous study on the copper(II)-L-dopa complex it was suggested that hydroxy groups on the phenyl moiety form hydrogen bonds with the inner-sphere water molecules of the metal ion, thereby misorienting the incoming ligand with respect to substitution.[5] A number of other studies on amino acid ligands with hydroxy groups have now been carried out,[4,6,17] some of which show the reduction in substitution rate constant. Since it is unlikely that the water-exchange rate constant is influenced by the presence or absence of this group at a site remote from chelation, a more likely explanation involves the reaction step of free ions to ion pair.

The ion-pair formation constant can be calculated from the quotient of the diffusion-controlled ion-pair association and dissociation rate constants.[18] Two possibilities should then be considered: hydrogen bonding reduces the association rate constant by cutting down the solid angle of approach to a value less than 4π, and hydrogen bonding increases the dissociation rate constant. Either effect leads to reduced values of K_{ip}, thus lowering k_1.

Studies with space-filling models show that hydrogen-bonding through the metal hydroxy group tends to rotate the amino acid end of the L-dopa molecule away from the metal ion. This misorientation would have the effect of increasing the distance of closest approach, a, between the metal ion and the negative charge center on the ligand. The ion-pair dissociation rate constant, however, is a complicated function of this parameter. Thus, in the absence of charge effects, larger values of a yield smaller dissociation rate constants, as this constant is proportional to $1/a^3$. For oppositely charged ions, on the other hand, an increase in a reduces the coulombic attraction, which leads to larger dissociation rate constants. Essentially, these effects compensate for each other. We conclude, therefore, that the observed effect is primarily due to a reduction in the number of successful encounters leading to ion-pair formation.

It is interesting that not all the amino acids containing hydroxyl groups display the anomalous kinetic behavior shown by L-dopa and hydroxyproline. Indeed, it has been postulated that hydrogen bonding in the ion pair between certain polyamines and coordinated waters increases complex formation rate constants.[19] These facts suggest that the nature and steric requirements of the ligand can play an important role in the kinetics of complexation, even though water loss is the rate-determining step.

Registry No. L-Dopa, 59-92-7.

Appendix

In the case of nickel, the relaxation spectrum is calculated from the solution of the two linear differential rate equations describing the system. In order to obtain these two linearly independent equations in two variables, it is sufficient to apply mass balance on ligand, metal, indicator, and proton together with the expanded protolytic equilibrium quotients for ligand and indicator. Well-known procedures incorporating these eight relations yields eq 2 and 3. The previously undefined terms are

$$R = [Ni^{2+}]\alpha_1 + [H_2L^-] - \frac{[Ni^{2+}]\alpha_2([NiHL]\alpha_3 + K_M)}{[NiHL]\alpha_4 + [H^+] + K_M} \qquad (A1)$$

---

(17) R. L. Karpel, K. Kustin, A. Kowalak, and R. F. Pasternack, *Biochim. Biophys. Acta*, **177**, 434 (1969).

(18) See ref 12b, p 63.

(19) D. B. Rorabacher, *Inorg. Chem.*, **5**, 1891 (1966).

$$S = \frac{[\mathrm{NiHL}](\alpha_4 - \alpha_3) + [\mathrm{H}^+]}{[\mathrm{NiHL}]\alpha_4 + [\mathrm{H}^+] + K_\mathrm{M}} \tag{A2}$$

$$\alpha_1 = \left(\frac{[\mathrm{HL}^{2+}]}{[\mathrm{H}^+]} + \frac{[\mathrm{H_2L}^-]}{K_{2\mathrm{a}}} + 4\frac{[\mathrm{H_3L}]}{K_{3\mathrm{a}}} + 1 + \frac{[\mathrm{In}] + [\mathrm{H}^+] + K_\mathrm{In}}{[\mathrm{H}^+] + K_\mathrm{In}}\right)\bigg/\sigma \tag{A3}$$

$$\sigma = \left(1 + \frac{[\mathrm{In}] + [\mathrm{H}^+] + K_\mathrm{In}}{[\mathrm{H}^+] + K_\mathrm{In}}\right)\left(1 + \frac{K_{1\mathrm{a}}}{[\mathrm{H}^+]} + \frac{[\mathrm{H}^+]}{K_{2\mathrm{a}}} + \frac{[\mathrm{H}^+]^2}{K_{2\mathrm{a}}K_{3\mathrm{a}}}\right) + \frac{[\mathrm{HL}^{2-}]}{[\mathrm{H}^+]}\left(1 + 2\frac{[\mathrm{H}^+]}{K_{2\mathrm{a}}} + 3\frac{[\mathrm{H}^+]^2}{K_{2\mathrm{a}}K_{3\mathrm{a}}}\right) + 2\frac{[\mathrm{H_2L}^-]K_{1\mathrm{a}}}{K_{2\mathrm{a}}[\mathrm{H}^+]} - \frac{[\mathrm{H_2L}^-]}{K_{2\mathrm{a}}}\left(\frac{[\mathrm{H}^+]^2}{K_{2\mathrm{a}}K_{3\mathrm{a}}} - 1\right) + 2\frac{[\mathrm{H_3L}]}{K_{3\mathrm{a}}}\left(3\frac{K_{1\mathrm{a}}}{[\mathrm{H}^+]} + \frac{[\mathrm{H}^+]}{K_{2\mathrm{a}}} + 2\right) \tag{A4}$$

$$\alpha_2 = \left(\frac{[\mathrm{HL}^{2-}]}{[\mathrm{H}^+]} - \frac{[\mathrm{H_2L}^-]}{K_{2\mathrm{a}}} - 2\frac{[\mathrm{H_3L}]}{K_{3\mathrm{a}}}\right)\bigg/\sigma \tag{A5}$$

$$\alpha_3 = \left(\frac{K_{1\mathrm{a}}}{[\mathrm{H}^+]} - \frac{[\mathrm{H}^+]}{K_{2\mathrm{a}}} - \frac{[\mathrm{H}^+]^2}{K_{2\mathrm{a}}K_{3\mathrm{a}}}\right)\bigg/\sigma \tag{A6}$$

$$\alpha_4 = \left(1 + \frac{K_{1\mathrm{a}}}{[\mathrm{H}^+]} + \frac{[\mathrm{H}^+]}{K_{2\mathrm{a}}} + \frac{[\mathrm{H}^+]^2}{K_{2\mathrm{a}}K_{3\mathrm{a}}}\right)\bigg/\sigma \tag{A7}$$

If the first term in eq A4 is much greater than the others, it is clear that the expression for α_4 reduces to

$$\frac{1}{1 + \dfrac{[\mathrm{In}] + [\mathrm{H}^+] + K_\mathrm{In}}{[\mathrm{H}^+] + K_\mathrm{In}}}$$

as in eq 2 in the text.

For cobalt, the single relaxation time is calculated analogously from the linear differential rate equation in one variable.

The previously undefined α term is

$$\alpha = \frac{\gamma K_{1\mathrm{a}} - \epsilon[\mathrm{HL}^{2-}]}{\gamma[\mathrm{H}^+]} + \frac{\gamma[\mathrm{H}^+] + \epsilon[\mathrm{H_2L}^-]}{\gamma K_{2\mathrm{a}}} + \frac{\gamma[\mathrm{H}^+]^2 + 2\epsilon[\mathrm{H}^+][\mathrm{H_2L}^-]}{\gamma K_{2\mathrm{a}}K_{3\mathrm{a}}} \tag{A8}$$

where

$$\gamma = 1 + \frac{[\mathrm{In}] + [\mathrm{H}^+] + K_\mathrm{In}}{[\mathrm{H}^+] + K_\mathrm{In}} + \frac{[\mathrm{HL}^{2-}]}{[\mathrm{H}^+]} + \frac{[\mathrm{H_2L}^-]}{K_{2\mathrm{a}}} + 4\frac{[\mathrm{H_3L}]}{K_{3\mathrm{a}}} \tag{A9}$$

$$\epsilon = \frac{K_{1\mathrm{a}}}{[\mathrm{H}^+]} - \frac{[\mathrm{H}^+]}{K_{2\mathrm{a}}} - 2\frac{[\mathrm{H}^+]^2}{K_{2\mathrm{a}}K_{3\mathrm{a}}} \tag{A10}$$

Contribution from the Department of Chemistry,
Purdue University, West Lafayette, Indiana 47907

Kinetics and Mechanism of the Oxidation of Cobalt(II) Aminopolycarboxylate Complexes by Hypobromous Acid and Hypobromite Ion

W. H. WOODRUFF, D. W. MARGERUM,* M. J. MILANO, H. L. PARDUE, and R. E. SANTINI

Received October 26, 1972

The oxidation of $[\mathrm{Co^{II}L}]^{2-}$ (L is ethylenediaminetetraacetate, EDTA^{4-}, and *trans*-1,2-diaminocyclohexane-*N,N,N',N'*-tetraacetate, CyDTA^{4-}) by bromine is studied as a function of pH. As the pH is increased, the identity of the kinetically important oxidant changes from a mixture of $\mathrm{Br_2}$ and $\mathrm{Br_3}^-$ to HOBr and finally to OBr^-. The reactions are first order in $[\mathrm{Co^{II}L}]^{2-}$ concentration and first order in the bromine species. The values of the rate constants (M^{-1} sec^{-1}) for the oxidations by $\mathrm{Br_2}$, HOBr, and OBr^- when L is EDTA are 7.3×10^{-2}, 65, and 2000, respectively, and when L is CyDTA, the values are 2.0×10^{-3}, 0.16, and 49, respectively. The product of the oxidation of $[\mathrm{Co^{II}L}]^{2-}$ by HOBr and OBr^- is either $[\mathrm{Co^{III}(L)OH_2}]^-$ or $[\mathrm{Co^{III}(L)OH}]^{2-}$, depending upon pH. Postoxidation ring closure gives $[\mathrm{Co^{III}L}]^{2-}$ where L is six-coordinate. This is a fast process for CyDTA and a rapid scan spectrophotometer is used to observe the oxidation and ring closure steps.

Introduction

The cobalt(II) complexes of EDTA and CyDTA, $[\mathrm{Co^{II}L}]^{2-}$, are oxidized by bromine species in aqueous solution as shown in eq 1. The reactions are first order in $[\mathrm{Co^{II}L}]^{2-}$ concentration and first order in $[\mathrm{Br_2}]_\mathrm{T}$, where $[\mathrm{Br_2}]_\mathrm{T} = [\mathrm{Br_2}] + [\mathrm{Br_3}^-] + [\mathrm{HOBr}] + [\mathrm{OBr}^-]$. The rate constants due to the various bromine species are designated in eq 2-5, and these four rate constants can be evaluated by variation of pH and the bromide ion concentration. The kinetics and mechanism of the oxidation of $[\mathrm{Co^{II}L}]^{2-}$ by $\mathrm{Br_2}$ and $\mathrm{Br_3}^-$ are reported elsewhere.[1] The present paper describes the study of reaction 1 as a function of pH, in order to determine the kinetics and mechanism of the oxidation of $[\mathrm{Co^{II}L}]^{2-}$ by HOBr and OBr^-.

$$2[\mathrm{Co^{II}L}]^{2-} + \begin{bmatrix} \mathrm{Br_3}^- \\ \uparrow\downarrow \\ \mathrm{Br_2} + \mathrm{Br}^- \\ \uparrow\downarrow \\ \mathrm{HOBr} + 2\mathrm{Br}^- + \mathrm{H}^+ \\ \uparrow\downarrow \\ \mathrm{OBr}^- + 2\mathrm{Br}^- + 2\mathrm{H}^+ \end{bmatrix} \rightarrow 2[\mathrm{Co^{III}L}]^- + 3\mathrm{Br}^- \tag{1}$$

$$[\mathrm{Co^{II}L}]^{2-} + \mathrm{Br_2} \xrightarrow{k_1} \text{products} \tag{2}$$

$$[\mathrm{Co^{II}L}]^{2-} + \mathrm{Br_3}^- \xrightarrow{k_2} \text{products} \tag{3}$$

$$[\mathrm{Co^{II}L}]^{2-} + \mathrm{HOBr} \xrightarrow{k_3} \text{products} \tag{4}$$

$$[\mathrm{Co^{II}L}]^{2-} + \mathrm{OBr}^- \xrightarrow{k_4} \text{products} \tag{5}$$

---

[1] W. H. Woodruff, B. A. Burke, and D. W. Margerum, to be submitted for publication.